Theoretical investigation of molecular and electronic structures of buckminsterfullerene-silicon quantum dot systems

A.S. Fedorov,[1,2]* A.A. Kuzubov,[2] A. Kholtobina,[2] E. A. Kovaleva,[2] J. Knaup,[3]* S. Irle[4]

[1]*Institute of Physics, Academy of Sciences, 660036, Krasnoyarsk, Russia*

[2]*Siberian Federal University, 660041, 79 Svobodny Prospect, Krasnoyarsk, Russia*

[3]*Bremen Center for Cormputational Materials Science, University of Bremen, 28359 Bremen, Germany*†

[4]*Institute of Transformative Bio-Molecules (WPI-ITbM) & Department of Chemistry, Graduate School of Science, Nagoya University, Nagoya 464-8602, Japan*

Abstract

Theoretical simulations of embedding and relaxation of buckminsterfullerene C_{60} molecules chemisorbed on representative surfaces and inside a bulk silicon lattice were performed using both the generalized gradient density functional theory (GGA-DFT) and the self-consistent-charge density-functional tight-binding (DFTB) molecular dynamics (DFTB/MD) methods. We chose fullerene molecules as representative models for general quantum dots on the surface or inside bulk a semiconductor, in this case silicon. If a single C_{60} molecule is chemisorbed on (001) and (111) silicon slab surfaces, static GGA-DFT calculations show that the C_{60} molecule deformation was very small and the C_{60} binding energies were roughly around 4 eV. In these configurations, the analysis of the charge distributions shows that the charge of C_{60} molecules on the (001) and (111) silicon surfaces was only between -2 to -3.5 electrons, respectively, that is correlates well with number of C-Si bonds linking the fullerene molecule and the silicon surface. On the other hand, static

†Current address: Atotech Deutschland GmbH, 10553 Berlin, Germany

GGA-DFT calculations of C_{60} molecule relaxation inside suitable hollow spheres in the bulk silicon were performed. After the silicon bulk-C_{60} system relaxation, we investigated electronic density of states (DOS), partial DOS and charge distribution. These calculations confirm that the C_{60} molecule remains stable inside bulk silicon having deformation energy values of between 11 and 15 eV for geometries with different rotational C_{60} configurations, respectively. Formation of some C-Si bonds cause local silicon amorphization and corresponded electronic charge uptake on the embedded fullerene cages. According to epy charge analysis, these quantum dots can accept up to 20 excess electrons, wherein while the main charge contribution is located on the carbon atom bonded to silicon atoms. The dynamic embedding process was modeled using the DFTB/MD method by placing a C_{60} molecule on top of a Si (111) slab surface and further exposition to a stream of silicon dimers with kinetic energies equivalent to a temperature of ~723 K directed to the C_{60}-silicon surface. After the final MD shot, the resulting geometry was fully relaxed. These calculations show that during landing of the C_{60} molecule on the silicon surface and subsequent overgrowth by silicon, C_{60} molecule remains stable inside bulk silicon, wherein the C_{60} molecule adopts a deformation energy of about 17.8 eV and the overgrowth process leads to a local silicon amorphization, in qualitatively good agreement with the static GGA-DFT calculations.

Keywords: fullerene, silicon, quantum dots, DFT theory, DFTB calculations, molecular dynamics, crystal structure growth

1. Introduction

Quantum dots(QD) have attracted considerable interest in the past few decades due to their high potential for use in microelectronic, optoelectronic or thermoelectric applications and even in quantum computing. Usually for electronic nanodot construction semiconductive materials are used. For example, pure silicon, hydrogen-capped silicon Si_mH_n and metal silicide nanoparticles exhibit high fluorescence and stimulated emission.[1,2]Unfortunately, quantum dots (QDs) usually have wide size distributions and therefore different electronic/optical properties. That is why QDs having equal sizes are very desirable for technological applications.

For this reason fullerene molecules, especially the most frequently produced buckminsterfullerene C_{60} molecule, is highly promising for use in the context of QDs. Fullerenes possess unique mechanical properties, chemical inertness and large interaction with an electromagnetic field. The use of fullerenes as QDs requires to isolate them from each other, which can and has been done frequently by placing them inside some matrix.[3,4]

Chemical and physical properties of fullerenes, especially those of the buckminsterfullerene C_{60}, have been the subject of intensive studies since its discovery in 1985. These molecules and their composite materials are considered as promising materials in various research areas, such as drug delivery systems, nano-(opto)electronics, fuel cell technology, photovoltaic cells, tribology and field emission technology. In references[3] and [4] the authors described the feasibility of fabricating of a single layer of C_{84} fullerene embedded on a Si (111) surface through a controlled self-assembly mechanism in an ultrahigh vacuum (UHV) chamber. The characteristics of the fullerenes embedded Si surface were investigated directly using UHV Scanning Tunneling microscopy (STM). STM has proven itself to be an excellent tool for the analysis of the adsorption of fullerenes

on varying surfaces and their interaction with these surfaces. This study demonstrated that a highly uniform single layer of the fullerene embedded (111) surface is formed due to self-assembly mechanism which has superior properties for nanotechnology applications. It has a high emission efficiency and a low turn-on voltage, making it highly promising as a field emitter source. STM I-V measurement shows that the embedded C_{84} molecules have a wide band gap of ~3.4 eV.

In reference 5, C_{60} molecules were deposited on a Si (001) surface with the formation of flat thin films consisting of C_{60}, having thicknesses varying from a few to 25 nm. By measuring the friction force vs. applied force for the Si (001) surface it was shown that the friction coefficient is decreased for more than one order of magnitude while silicon surface is covered by a C_{60} thin film. There are some experimental works devoted to investigation of C_{60} molecules implanted in porous silicon.[6-8]In reference [6] the authors observed an enhanced photoluminescence (PL) signal, in addition to the PL peak of porous Si, a peak at 730 nm caused by perfect C_{60} molecules and other peaks at 620 and 630 nm caused by imperfect C_{60} molecules. In the same work, unusual Raman features related to the C_{60} molecular environments and disorder effects inside solid silicon were obtained with large intensities. Particularly, a downshift of the pinch A_g mode, sensitive to the charge on the C_{60} was observed by more than 12 cm^{-1}, indicating a charge transfer of at least 2 electrons per C_{60} molecule in the samples. Yet, despite the significant number of works devoted to the experimental measurement of the optical characteristics of fullerene-porous silicon systems, the theoretical description of geometric and electronic structure of fullerene molecules inside the porous silicon is absent. Also there is only a very limited number of theoretical studies of fullerene covering on the silicon surfaces, one for instance reported in reference [3], where properties of C_{84} film were calculated using periodic density functional theory (DFT) calculations. Unfortunately, the C_{84} film was modeled without silicon

covering due to limited computational resources, and the study is therefore insufficient to discuss the issue of charge transfer from silicon to the fullerene QDs. Therefore, we have here investigated the molecular and electronic structure of isolated C_{60} fullerene in a cavity inside bulk silicon as well as the properties of regular C_{60} covering on the (001) and (111) periodical silicon slab surfaces by static DFT calculations and quantum chemical molecular dynamic (MD) based on an approximate DFT potential.

2. Computational Details

The density functional theory (DFT)[8,9] based calculations were carried out using the Vienna Ab initio Simulation Package (VASP).[10,11]In these calculations, a projector augmented wave method (PAW) was selected to best describe electron wavefunctions and the interactions between an ion core and valence electrons.[12] The plane wave basis cut off energy was set to 400 eV. The exchange-correlation terms were taken into account using the Perdew-Berke-Ernzerhof form of the GGA.[13] The k-point sampling in the first Brillouin zone (1BZ) was chosen according to the Monkhorst-Pack scheme[14] using different choices for the number of k points as indicated below. Geometry optimizations were carried out until forces acting on all atoms in all structures became smaller than 0.05 eV/A. Atomic charges were computed using Bader charges on numerical grids as described in reference 15.

The quantum chemical MD simulations of C_{60} molecule overgrowth were performed on-the-fly using the DFTB method,[16] employing its self-consistent-charge version[17] (recently referred to as DFTB2). The well-tested pbc-0-3 set[18] of DFTB Slater-Koster and repulsive potential parameters was employed for these calculations, and electronic self-consistency was iteratively obtained until occupations differed only by $\leq 10^{-8}$ electrons

between iterations. Electronic occupation was determined according to a Fermi-Dirac distribution at 723 Kelvin. The ionic equations of motion were solved using the velocity form of the Velocity-Verlet algorithm using a time integration step of 0.5 fs. Static DFTB geometry optimizations were iterated until the atomic forces fell below 10^{-5}H/Bohr (~$5x10^{-4}$ eV/A).

3. Results and Discussion

3.1. Modeling of C_{60} molecules chemisorbed on the silicon (001) surface

The silicon (001) surface was modeled by a periodical slab using supercell sizes8.628×8.628×12.942 Å, which correspond to a silicon layer that is 12 atom layers thick. Before the C_{60} molecule was placed atop, the experimentally observed 2×1 dimer surface reconstruction was simulated. This reconstruction allowed to reduce number of dangling bonds on the surface by the dimer formation. After that the fullerene molecule was placed above the slab surface and system was fully optimized using GGA-DFT. During the optimization, a 6×6×1Monkhorst-Pack k-point mesh was used. Taking into account the supercell sizes, the distance between neighboring fullerenes was 8.63 Å. At that vacuum space between top of the C_{60} molecule and the nearest image of the silicon slab was 11.25 Å in vertical direction. Two structures were investigated with different initial fullerene placement: a structure without of C_{60} molecule rotation relative to Si dimers and the structure with 90^{o} rotation, as shown in Fig. 1.

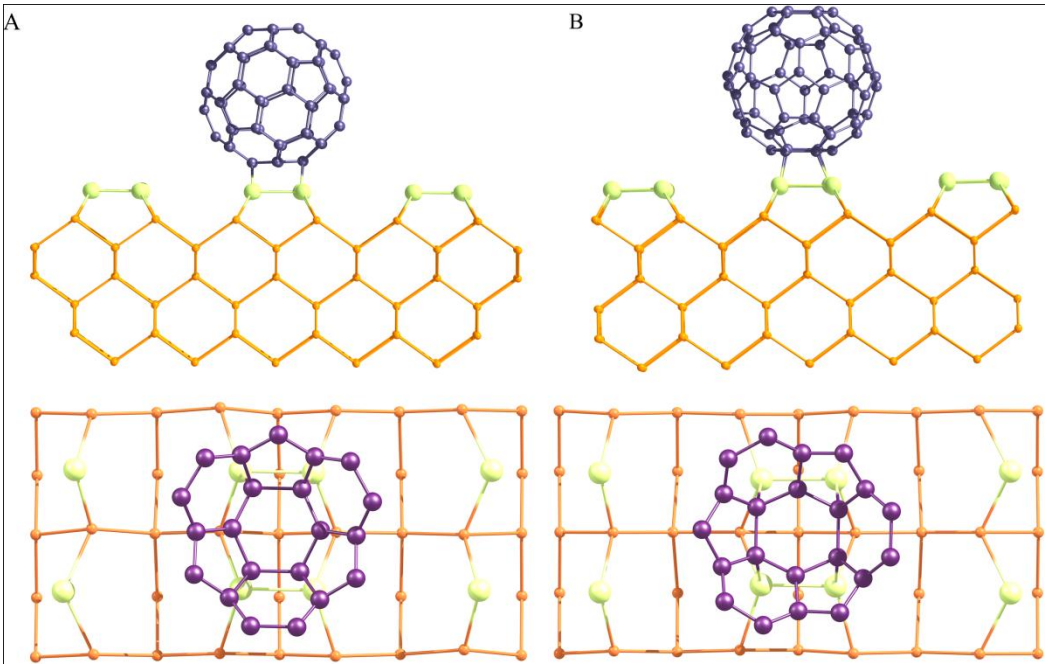

Figure 1. Top and side view of relaxed C_{60} fullerenes atop reconstructed Si (001) surface: Panel A— first geometry; Panel B— geometry after 90^{o}rotation of the fullerene molecule. The green spheres represent the silicon atoms located on the surface.

The calculated binding energies, -3.61 and -4.28 eV for the first and for the second structures correspondingly, show that the second type of deposition is more likely to occur. Bader charge analysis[15]predicts that the fullerene total charge uptake in the second deposition mode was equal to -3.58 electrons, owing to the difference in the levels of Fermi of the silicon slab and the fullerene molecule.

In Fig. 2, panel A, the electronic density of states (DOS) and different partial DOS (pDOS) for this favorable geometry are shown. This figure demonstrates that the combined system has conductive properties due to silicon and fullerene's high levels of DOS near the Fermi level. Panel B shows the difference of partial DOS (pDOS) of silicon atoms on the surface with and without the fullerene molecule. Panel C shows the difference of pDOS of

the fullerene atoms for the standalone C_{60} molecule and for the C_{60} molecule on the (001) silicon surface.

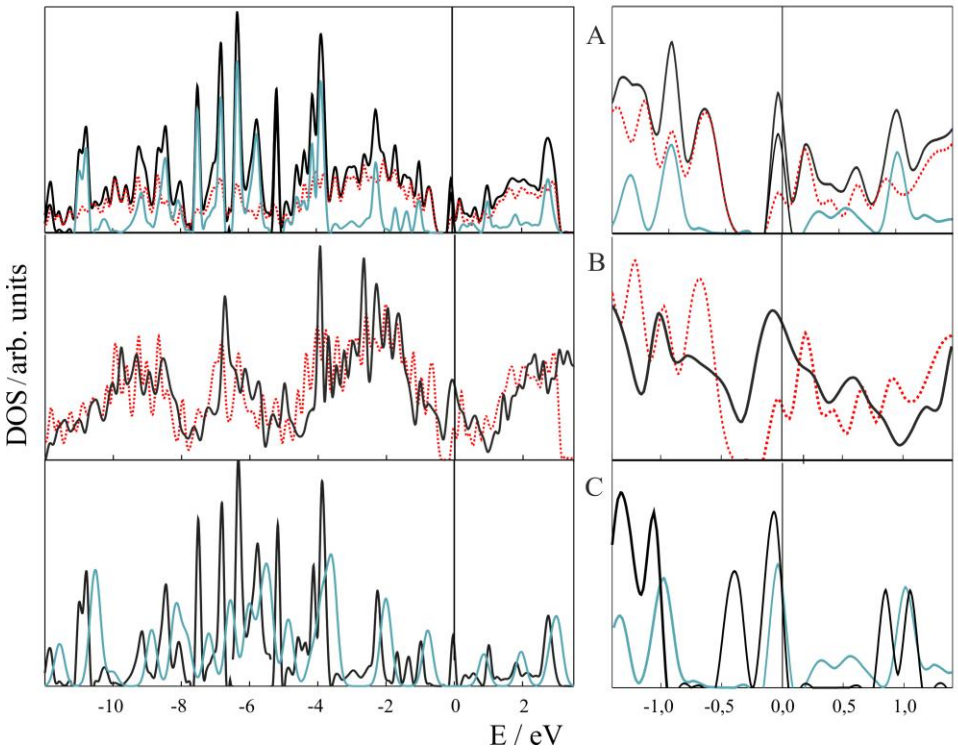

Figure2. Total DOS and pDOS for the C_{60} molecules chemisorbed on the silicon (001) 2×1 reconstructed surface. Panel A: black lines – total DOS, red lines – pDOS corresponded to Si atoms, blue lines –pDOS corresponded to the fullerene molecule on the surface; Panel B: red line –pDOS of silicon atoms on the surface with the fullerene molecule; black line – pDOS of silicon atoms on the surface without the fullerene molecule; Panel C: black line – DOS of the standalone C_{60} molecule, blue line – pDOS of the fullerene's atoms on the surface.

3.2. Modeling of C_{60} molecules chemisorbed on the (111) silicon surface

The silicon (111) surface was modeled by a periodical slab using supercell sizes 11.601×11.601×18.910 Å, which corresponds to a 12 atom layer slab thickness with a

fullerene-fullerene distance of 11.60 Å. Because of experimentally there is not dimer formation on this surface, we did not use dimer reconstruction of this surface. Initial normal to the surface atom displacements we did not considered because of at the surface and fullerene contact these displacements were inevitably changed with the formation of Si-C bonds. The slab surface opposite to the fullerene's molecules surface was passivated by hydrogen atoms, to eliminate the influence of the unpaired electrons of the surface. The vacuum space between top of the C_{60} molecules and the nearest image of the silicon slab in vertical direction was 12.35 Å. Three different positions of C_{60} on Si (111) were considered and are energetically most favorable: a position "bond" where fullerene atoms (1,6) have 2 neighboring Si atoms in the upper silicon (Panel A); a position "hex" where fullerene atoms (1,4) of opposite hexagon vertexes are bonded with 2 Si atoms of the upper layer (Panel B); finally a position "trig" where fullerene atoms (1,3,5) of alternate hexagon vertexes are bonded with 3 Si atoms of the upper layer (Panel C), see Fig. 3.

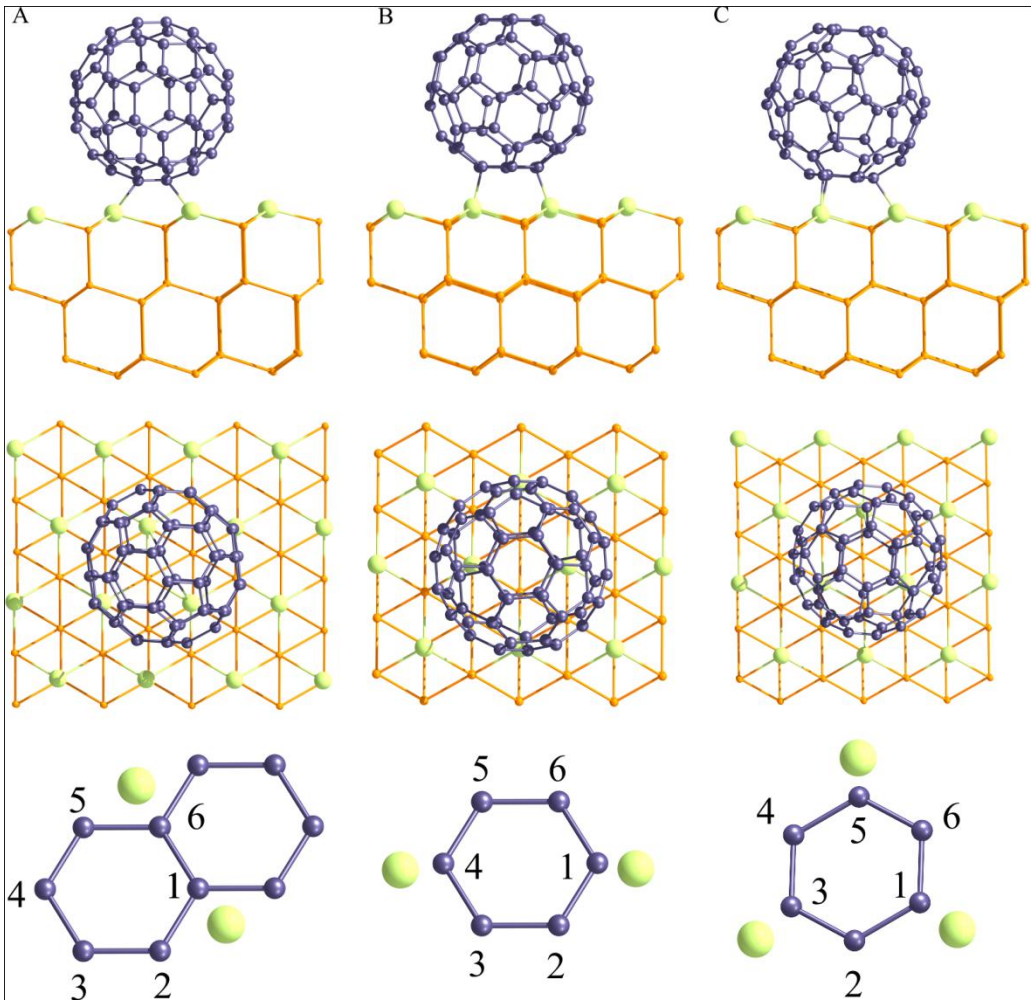

Figure 3. Top and side view of relaxed C_{60} fullerenes atop reconstructed Si(111) surface "bond"(A) , "hex"(B) and "trig"(C). The green spheres represent the silicon atoms Si atoms in the upper silicon.

The structures were optimized and the binding energies were calculated with a 3×3×1 Monkhorst-Pack k-point mesh. The GGA-DFT binding energies for "hex", "bond" and "trig" structures were -3.57,-2.93 and-2.75 eV correspondingly. The DOS was calculated for the most stable "hex" structure (see Fig 4; the arrangement of panels is similar to Fig. 2).

In Fig. 4 the electronic density of states (DOS) and different partial DOS (pDOS) for this favorable geometry are shown. Panel B shows differences of pDOS of silicon atoms on the surface with and without the fullerene molecule. Panel C shows the difference of pDOS of the fullerene atoms for the standalone C_{60} molecule and for the C_{60} molecule on the (111) silicon surface. The Bader charge analysis indicates that the fullerene total charge -2.05 electrons for the most favorable "hex" geometry.

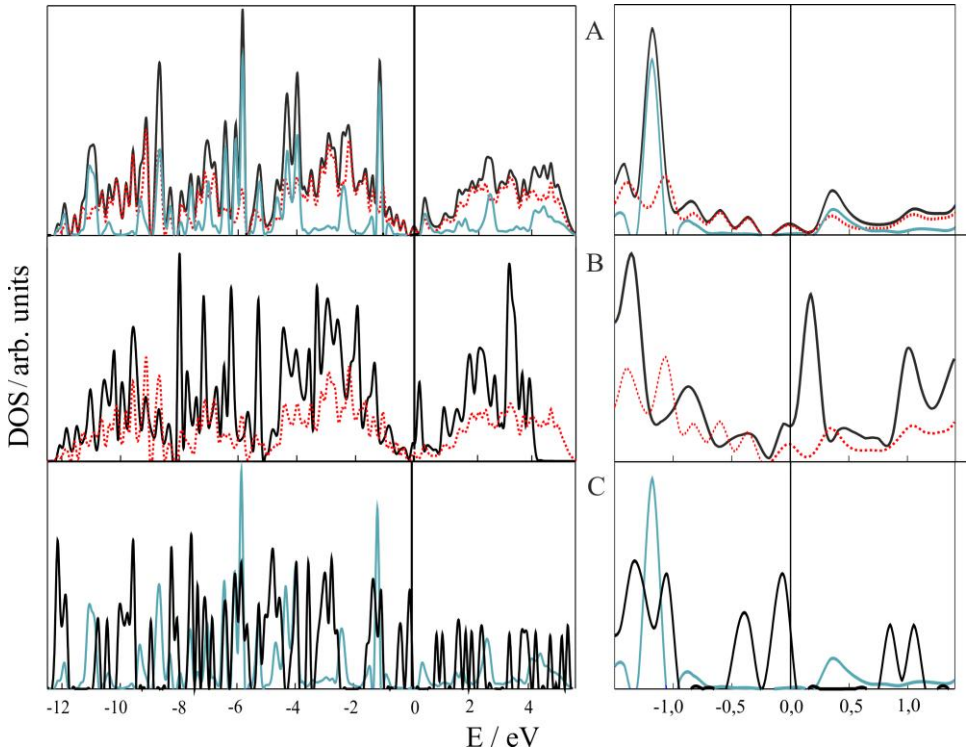

Figure 4. Total DOS and pDOS for the C_{60} molecules chemisorbed on the silicon (111) surface. Panel A: black lines – total DOS, red lines – pDOS corresponding to Si atoms, blue lines – pDOS corresponding to the fullerene molecule on the surface; Panel B: black line – DOS of silicon surface without the fullerene, red line –pDOS of silicon atoms on the surface with the fullerene molecule; Panel C: black line – DOS of standalone C_{60}, blue line – pDOS of the fullerene's atoms in the structure.

In Table 1 the binding and deformation energies of the C_{60} molecule with silicon (001) and (111) surfaces are shown for different geometries. The fullerene binding energies E_{bond} have been calculated as: $E_{bond}=E_{structure}-E_{full}- E_{si\_slab}$, where $E_{sucture}$– total energy of complex system (slab+ C_{60} molecule on the surface), E_{full}-total energy of the optimized isolated C_{60} molecule, E_{si_slab} -total energy of the silicon slab;

The C_{60} molecule deformation energies E_{deform} have been calculated as: $E_{deform}=E_{full\_si}-E_{full}$, where E_{full}–total energy of the optimized isolated C_{60} molecule; E_{full_si}– total energies of isolated fullerene molecule having the same geometry as the molecule on the slab surface.

Table 1. Binding and deformation energies of the C_{60} molecule chemisorbed on the (001) and (111) silicon slab surfaces for different geometries.

Structure	Binding energy (eV)	Deformation energy (eV)
Si(001)_0^O	-3.61	5.51
Si(001)_90^O	-4.28	5.16
Si(111)_hex	-3.57	4.58
Si(111)_bond	-2.93	4.80
Si(111)_trig	-2.75	4.35

3.3. Modeling of C_{60} molecules embedded inside bulk silicon

As mentioned above, we also investigated the C_{60} molecule embedded inside a periodic silicon supercell using GGA-DFT geometry optimizations. In the supercell of sizes 12.942 × 12.942 × 12.942a spherical cavity of 8.60 Å diameter was created, in which one

C_{60} molecule was placed. The 1BZ integration was performedusinga2×2×2 Monkhorst-Pack k-point mesh.

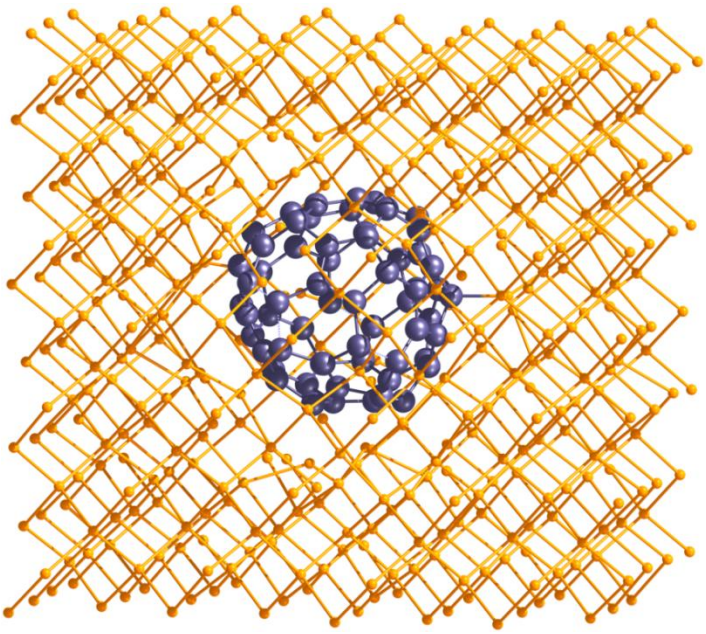

Figure 5. GGA-DFT optimized atomic structure of crystalline silicon with an embedded C_{60} fullerene molecule (geometry C_{60}Si_1).

To verify the optimized geometry depending on the initial fullerene position inside the cavity, the fullerene was rotated by0°, 10° and 20° relative TO the cavity (geometries C_{60}Si_1, C_{60}Si_2, C_{60}Si_3 correspondently). To optimize the whole system geometry, a damped molecular dynamic method was employed within the GGA-DFT method, using a damping factor of μ=0.01. During geometry optimization, no additional rotation of the buckminsterfullerene molecule was observed. After optimization, the shortest Si-C bond lengths were found to be 1.732, 1.757 and 1.732 Å for these geometries, respectively, which are comparable to the bond length Si-C in silicon carbide (1.88 Å). One of the optimized geometries is shown on Fig. 5.

Fig. 6 shows the DOS for the three studied structures. One can see that the rotation of the fullerene does not affect to the DOS significantly, so we assume these DOS correctly describes electronic properties of single C_{60} molecule embedded inside bulk silicon. The DOS value on the Fermi level shows that the fullerene penetration into bulk silicon leads to the system conductive properties and silicon amorphization due to weak Si-C bond formation, while the number of such interactions easily allows for the overall deformation of the C_{60} cage structure.

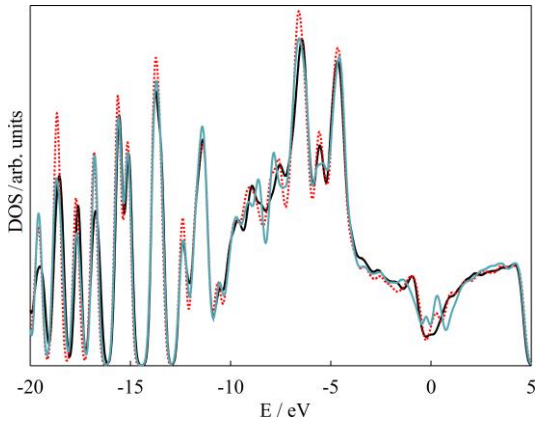

Figure 6. DOS for bulk silicon with embedded the C_{60} fullerene molecule for geometry $C_{60}Si\_1$ (black line), $C_{60}Si\_2$ (red line), $C_{60}Si\_3$ (blue line).

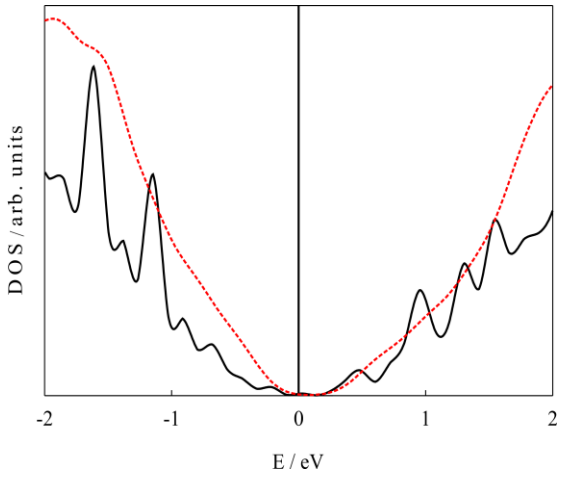

Figure 7. Comparison of partial DOS for maximally distant from the C_{60} molecule Si atom (black line) and total DOS of the bulk silicon (red line).

To check the Si-C bond formation effect, the partial DOS for the Si atom at maximum distance (9.81Å) from the C_{60} molecule was calculated, which is shown in Fig. 7. The figure shows that this pDOS is similar with DOS of perfect semi conductive bulk silicon. Thus, the system conductivity and amorphization is explained by formation of bonds between the fullerene molecule and nearest silicon atoms, which in turn weakens the C-C bonds of the fullerene cage.

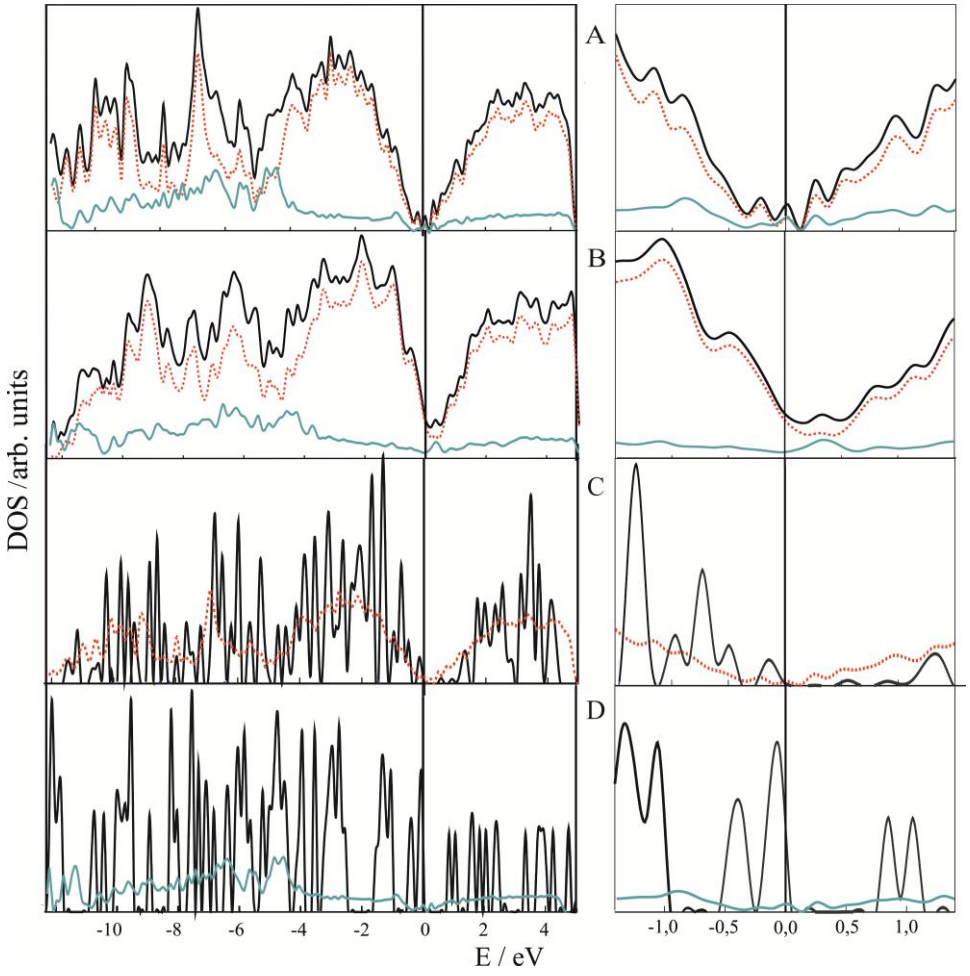

Figure8. Comparison of DOS and some partial DOS (pDOS) for bulk silicon with embedded (DFT optimization) or overgrown (nonequilibrium DFTB/MD simulation) C_{60}

fullerene molecule. Panel A:DFTB DOS for the optimized geometry of the overgrown C_{60}molecule during the DFTB/MD simulation (see below). Black lines – total DOS, red lines – pDOS of silicon atoms, blue lines – pDOS of overgrowed C_{60} molecule; Panel B: DOS for the GGA-DFT optimized geometry of the bulk silicon with the embedded C_{60} molecule during DFT optimization. Black lines – total DOS, red lines – pDOS of silicon atoms, blue lines – pDOS of embedded C_{60} molecule; Panel C: pDOS of silicon atoms for the optimized geometry of the bulk silicon with (red line) or without(black line) the embedded C_{60} molecule; Panel D: black line – DOS of standalone C_{60}, blue line – pDOS of fullerene atoms inside bulk silicon.

In Fig. 8, the total and different partial DOS for the isolated C_{60}molecule, bulk silicon and the bulk silicon with embedded the C_{60} fullerene molecule for geometry C_{60}Si_1are shown. These DOS, shown in Figure 8A, point to the system conductive properties due to the formation of Si-C bonds. These bond formations are reflected in the appearance of peaks near the Fermi level. Additional features in the silicon pDOS peaks when C_{60} molecule becomes embedded into bulk silicon reflects the silicon amorphization. Also there is broadening and blurring of the fullerene carbon pDOS peaks due to deformation of the highly symmetrical C_{60} molecule and its interaction with the bulk silicon atoms.

To describe the stability changes of the fullerene skeleton inside bulk silicon we used a method of determining the kinetic stability of nanostructures as suggested in reference 19. This method is based on the computation of the molecular destruction probability determined by the “probability of breaking chemical bonds” (PBCB) in a molecule due to thermal vibrations and stretching it to a certain critical value. To calculate the probability of this stretching, the central limit theorem and the assumption of independence phases of thermal vibrations were used together on the basis of normal

harmonic vibrational frequencies. One then assumes that the summation of probabilities of the chemical bonds breaking in the molecule (nanostructure) determines the probability of destruction of the entire molecule at a given temperature. Using this approach we computed the PBCB of the isolated C_{60} molecule and of the molecule inside bulk silicon. They were $0.54x10^{-11}$ and $3.14x10^{-6}$ respectively at temperature of 900 Kelvin. This result indicates that the fullerene molecule is much less stable inside bulk silicon due to the deformation of the C_{60} molecule and the weakening of its C-C bonds inside bulk silicon.

3.4. Results of DFTB/MD simulations and comparison with DFT calculations

The nonequilibrium DFTB/MD procedure of fullerene overgrowth by silicon to produce the C_{60} QD inside silicon was started by placing apreoptimizedC_{60} molecule on top of a 15.4x15.4 $Å^2$Si (111) slab model, with the C_{60} side being allowed to reconstruct and the opposite layers terminated by H atoms. After an initial pre-relaxation, the whole model was initialized to Boltzmann-distributed velocities according to a temperature of 723.15 K, with the bottom Si layer and terminating H atoms kept fixed.

Subsequently, groups of 4 to 5 Si_2 dimers, staggered 5 Å apart in surface normal direction and randomly placed laterally, were shot at the surface with a surface normal velocity component of 4.63Å/ps and a random lateral component of ~5% of that. Small variations to these parameters between shot groups ensured equal lateral Si distribution and avoided premature Si clustering before reaching the surface. In order to avoid detrimental thermostat influence on the incoming Si dimers, we employed the subsystem-thermostat approach described by Page *et al.*,[20] where only the moving part of the crystalline Si slab was set to a temperature of 723.15 K using an Andersen-type thermostat.

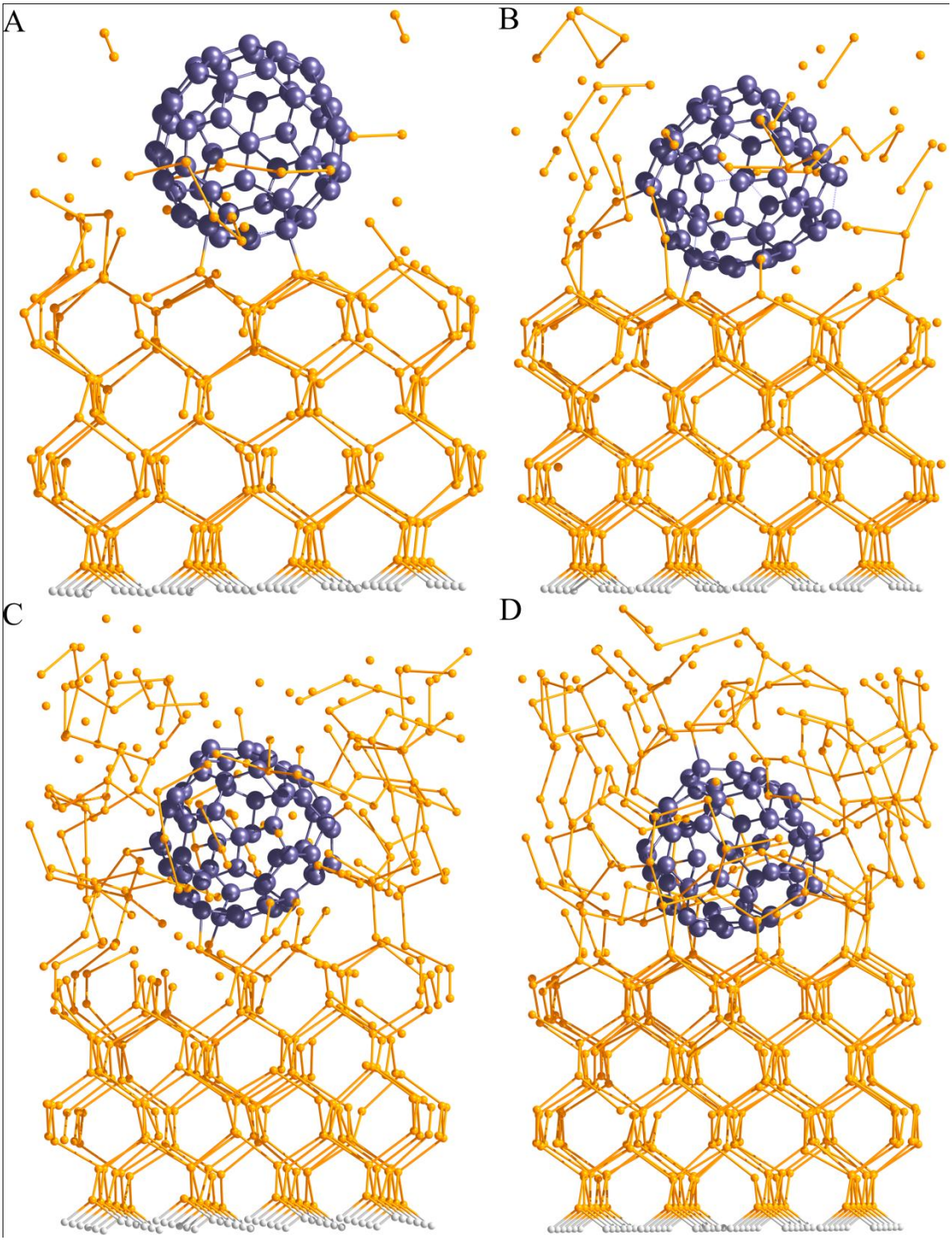

Figure9. Different stages of C_{60} fullerene overgrowth processon (111) silicon surface according to DFTB/MD simulation.

Fig.9 shows different stages of theC_{60}fullereneovergrowthprocess on the (111) silicon surface. Panels A-D show geometries after drops of 15, 27, 48 and 60 Si_2 dimers

onto the (111) silicon surface correspondently. For every geometry 6 to 10 ps MD time intervals were performed to allow thermalization of the newly incorporated atoms. After the final MD shot, the resulting geometry was relaxed using DFTB until the interatomic forces fell below 10^{-5} eV/A, see Fig. 9 D. To determine the deformation energy on the C_{60} fullerene inside bulk silicon, the C_{60} molecule was extracted and its total energy was calculated for this fixed geometry. Also the C_{60} total energy was calculated when all atoms positions were allowed to relax until forces acting to them became lower than 10^{-5}eV/A. After completion of the overgrowth process, using GGA-DFT calculations for the final geometry, DOS and pDOS (Fig. 8 A) and charge distribution (Table 2) were computed.

Table 2. Charges and deformation energies of C_{60} molecule inside bulk silicon. "C_{60}Si_DFTB" refers to the representative structure shown in Fig. 9 D.

Structure	Total C_{60} charge	C_{60} charge (per C atom)	C_{60} deformation energy(eV)
C_{60}Si_l	-19.97	-0.33	14.88
C_{60}Si_2	-17.40	-0.29	11.38
C_{60}Si_3	-19.38	-0.32	13.66
C_{60}Si_DFTB	-15.63	-0.26	17.75

Finally, one can see the embedding of the C_{60} molecule inside a hollow of bulk silicon leads to strong deformations of the carbon cage although the carbon connectivity remains intact. Short Si-C bonds are observed on the order of 1.7 Å, and fullerene molecule can take up to 20 excess electrons on its skeleton. This indicates a high population of π^* antibonding molecular orbitals, weakening the C-C bonds and causing a huge deformation energy of the cage on the order of 11 to 18 eV.

4. Conclusions

Using quantum chemical methods, we investigated the interaction of buckminsterfullerene C_{60} molecules with silicon in different configurations: chemisorption of the fullerene molecule on representative surfaces, and within the silicon bulk. Molecular and electronic structure calculations were performed using standard GGA-DFT methods, and the dynamic overgrowth process of a C_{60} molecule on a silicon (111) surface was modeled using nonequilibrium DFTB/MD simulations in which silicon dimers were periodically added on top of the surface and around the fullerene molecule. In all calculations, the isolated pentagon cage structure of the buckminsterfullerene molecules was preserved, indicating that C_{60} will retain its structural integrity when used as a quantum dot (QD) on silicon surfaces or placed in bulk silicon.

Chemisorption of buckminsterfullerene on a reconstructed (001) surface results in binding between the fullerene carbon atoms and the Si_2 surface dimers. The binding energies are approximately between -3.6 and -4.3 eV depending on the cage orientation, deformation energies of the fullerene were on the order of 5 eV, and electron transfer from the silicon surface to the fullerene molecule amounts to roughly 3 to 4 electrons. The chemisorption on the silicon (111) surface was generally less favorable, with a configuration we labeled “hex” being somewhat competitive with the weaker chemisorption configuration on the (001) surface. Overall, binding energies range from -2.8 to -3.6 eV, with deformation energies of the fullerene molecule being smaller by roughly 0.5 eV in comparison to the more stronger chemisorbed C_{60}-Si(001) system. The weaker interaction is also expressed in a smaller charge uptake by the fullerene molecule on the (111) surface, overall, only about 2 electrons are transferred in this case.

Embedding of the C_{60} molecule inside a hollow of bulk silicon leads to strong deformations of the carbon cage although the carbon connectivity remains intact. This is confirmed in dynamic simulations of silicon overgrowth where periodically Si_2 dimers were dropped on the surface and around the fullerene molecule. In these DFTB/MD simulations, we observed significant amorphization of the overgrown Si layers, possibly due to the fact that the MD simulation times were too short to allow for crystal structure healing and formation. Nevertheless, the general features of the DFT static calculations were also found in the DFTB/MD simulations: large electron take up by the fullerene molecule and a high deformation energy.

In conclusion, we predict that C_{60} molecules remain structurally intact even under harsh synthesis conditions at high temperatures, and that they can be used as highly negative quantum dots in bulk silicon with a wide spacing between them due to Coulombic repulsion.

Acknowledgment

The work was supported by Ministry of Education and Science of Russia (Russian-Japanese joined project, Agreement 14.613.21.0010, ID RFMEFI61314X0010).The authors are grateful to the Joint Supercomputer Center of Russian Academy of Sciences, Moscow and Siberian Supercomputer Center of SB RAS, Novosibirsk for the opportunity to use their computer clusters to perform the calculations. S.I. acknowledges partial support from a JST CREST grant.

References

1. Akcakir, O.; Therrien, J.; Belomoin, G.;Barry, N.; Muller, J. D.; Gratton, E. and Nayfeh, M., *Appl. Phys. Lett.* **2000**, *76*, 1857.

2. Belomoin,G.;Therrien, J.;Smith, A.; Rao, S.; Twesten, R.; Chaieb, S.; Nayfeh, M. H.; Wagner, L.; and Mitas, L., *Appl. Phys. Lett.* **2002**, *80*, 841-843.

3. Huang, W.; Su, C.;Chuan,S. and Ho, M.; *RSC Adv.* **2013**, *3*, 9234-9239.

4. Matsumoto, N.; Suzuki, H.;Kinoshita H.; Ohmae, N., *Tribology Online* **2008**, *3*(4), 232-237.

5. Yan, F.; Bao, X. M.;Wu, X. W.;Chen, H. I.,*Appl. Phys. Lett.***1995,** *67*, 3471-3473.

6. Wu. X. L.; Yan, F.; Bao, X. M.; Tong, S.; Siu, G. G.; Jiang, S. S.; Deng, F.,*Phys. Lett. A* **1997**, *225*, 170-174.

7. Wu, X. L.; Deng, Z. H.; Xue, F. S.; Siu, G. G.; Chu, P. K., *J. Chem. Phys.* **2006**, *124*, 214706/1-4.

8. Hohenberg, P.; Kohn, W., *Phys. Rev.* **1964,** *136*, 864-871.

9. Kohn, W.; Sham, L. J., *Phys. Rev.* **1965,** *140*, 1133-1138.

10. Kresse, G.;Hafner, J., *Phys. Rev. B* **1993**, *47*, 558-561.

11. Kresse, G.; Furthmüller, J., *Phys. Rev. B* **1996**, *54*, 11169-11186.

12. Blöchl, P. E., Phys. Rev. B **1994**, *50*, 17953-17979.

13. Perdew, J. P.; Burke, K.; Ernzerhof, M.; *Phys. Rev. Lett.* **1997**, *77*, 3865-3868.

14. Monkhorst, H. J.; Pack, J. D., *Phys. Rev. B* **1976,** *13*, 5188-5192.

15. Sanville, E.; Kenny, S. D.; Smith, R.: Henkelman, G., *J. Comp. Chem.* **2007,** *28*, 899-908.

16. Seifert, G.; Porezag, D.; and Frauenheim, Th., *Int. J. Quant. Chem.* **1996**, *58*, 185-192.

17. Elstner, M.; Porezag, D.; Jungnickel, G.; Elsner, J.; Haugk, M.; Frauenheim, Th.; Suhai, S.; Seifert, G., *Phys. Rev. B* **1998**, *58*, 7260-7268.

18. Rauls, E.; Gutierrez, R.; Elsner, J.; Frauenheim, Th., *Sol. State Comm.* **1999**, *111*, 459-464.
19. Fedorov, A. S.; Fedorov, D. A.; Kuzubov, A. A.; Avramov, P. V.; Nishimura, Y.; Irle, S.;Witek, H. A., *Phys. Rev. Lett.* **2011**, *107*, 175506/1-5.
20. Page, A. J.;Isomoto, T.; Knaup, J. M.; Irle, S.; Morokuma, K., *J. Chem. Theory Comput*. **2012**, *8*, 4019-4028.